# Phonon anomalies and electron-phonon interaction in the RuSr₂GdCu₂O₈ ferromagnetic superconductor: Evidence from infrared conductivity

A. V. Boris,[1,2] P. Mandal,[1,3] C. Bernhard,[4] N. N. Kovaleva,[2] K. Pucher,[1] J. Hemberger,[1] and A. Loidl[1]

[1]*Experimentalphysik V, EKM, Universität Augsburg, D-86135 Augsburg, Germany*

[2]*Institute of Solid State Physics, Russian Academy of Sciences, Chernogolovka, Moscow district 142432, Russia*

[3]*Saha Institute of Nuclear Physics, 1/AF, Bidhannagar, Calcutta 700 064, India*

[4]*Max-Planck-Institut für Festkörperforschung, Heisenbergstrasse 1, D-70569 Stuttgart, Germany*

Critical behavior of the infrared reflectivity of RuSr₂GdCu₂O₈ ceramics is observed near the superconducting $T_{SC}=45$ K and magnetic $T_M=133$ K transition temperatures. The optical conductivity reveals the typical features of the $c$-axis optical conductivity of strongly underdoped multilayer superconducting cuprates. The transformation of the Cu-O bending mode at 288 cm$^{-1}$ to a broad absorption peak at the temperatures between $T^*=90$ K and $T_{SC}$ is clearly observed, and is accompanied by the suppression of spectral weight at low frequencies. The correlated shifts to lower frequencies of the Ru-related phonon mode at 190 cm$^{-1}$ and the mid-IR band at 4800 cm$^{-1}$ on decreasing temperature below $T_M$ are observed. It provides experimental evidence in favor of strong electron-phonon coupling of the charge carriers in the Ru-O layers which critically depends on the Ru core spin alignment. The underdoped character of the superconductor is explained by strong hole depletion of the CuO₂ planes caused by the charge carrier self-trapping at the Ru moments.

## I. INTRODUCTION

The layered ruthenate-cuprate compound RuSr₂GdCu₂O₈ (Ru-1212) is a subject of intense interest as a unique model system to study the interplay between superconductivity and ferromagnetism. A ferromagnetic (FM) moment of the Ru-O layers coexists with superconductivity originating from the Cu-O bilayers over a broad temperature range.[1–5] Long-range magnetic order in Ru-1212 is established at $T_M$ = 133 K. Recent neutron-diffraction and magnetization studies[6,7] display that in zero external magnetic field the magnetic order of the Ru moments is predominantly antiferromagnetic along the $c$ axis with spin canting in the $ab$ plane. The net in-plane magnetic moment is most likely due to the rotations of the RuO₆ octahedra. It is suggested that there is a field-induced spin reorientation, and that already at moderate fields the order becomes predominantly ferromagnetic. At the same time dc transport and heat-capacity measurements show that Ru-1212 behaves as a typical underdoped cuprate superconductor with the onset of superconductivity at $T_{SC}=45$ K and clearly exhibits a number of features arising from the presence of a normal state pseudogap.[5]

The importance of $c$-axis charge dynamics for the high-$T_C$ superconductivity still remains controversial.[8,9] Many aspects of the $c$-axis transport properties of superconducting (SC) bilayer compounds such as YBa₂Cu₃O₇₋δ (Y-123) have been explained with a model invoking the onset of interbilayer and intrabilayer Josephson currents.[8,10,11] From this point of view, Ru-1212 presents a unique opportunity to investigate, how the SC Cu-interbilayer coupling propagates through magnetic RuO layers.

A more specific question concerns the hole doping of the CuO₂ planes required for the superconductivity in Ru-1212 compound. The hole doping obtained from bond-valence summations based on the refined crystal structure amounts to

$p\sim0.4$ per Cu atom, and results from an overlap of the Ru:$t_{2g}$ and the Cu:$3d_{x^2-y^2}$ bands.[3] However, the hole doping of the CuO₂ planes derived from dc transport and heat-capacity measurements points towards $p\sim0.1$.[5] This discrepancy probably reflects hole trapping and/or strong scattering by the ferromagnetic Ru moments.

The present work aims to address these issues by studying the critical behavior in the infrared (IR) optical conductivity of the Ru-1212 ceramics near the superconducting ($T_{SC}$) and magnetic ($T_M$) transition temperatures. The optical conductivity of Ru-1212 reveals the typical features of the $c$-axis optical conductivity of underdoped multilayer superconducting cuprates. Namely, the transformation of the Cu-O bending mode into an additional broad absorption peak below a characteristic temperature $T^*=90$ K, significantly above $T_{SC}$, which is accompanied by the relative suppression of the optical conductivity spectral weight at low frequencies. In addition, a distinct polaron-shaped band at about 4800 cm$^{-1}$ dominates the mid-IR conductivity. On decreasing temperature the increase of the total spectral weight associated with the intraband transitions is significantly enhanced below $T_M$. The correlated shifts of the phonon mode at 190 cm$^{-1}$ and the mid-IR band to lower frequencies below $T_M=133$ K provide experimental evidence in favor of strong electron-phonon coupling of the charge carriers in the Ru-O layers which is governed by the magnetic order.

## II. EXPERIMENTAL

Polycrystalline Ru-1212 samples were synthesized by solid-state reaction from high purity RuO₂, SrCO₃, Gd₂O₃, and CuO powders, as described in details elsewhere.[5,12] At the final stage of the preparation the sample in the form of a pressed pellet was annealed at 1060 °C for 6 days in flowing oxygen and was polished to optical quality. X-ray diffraction confirms that the sample is single-phased with a tetragonal
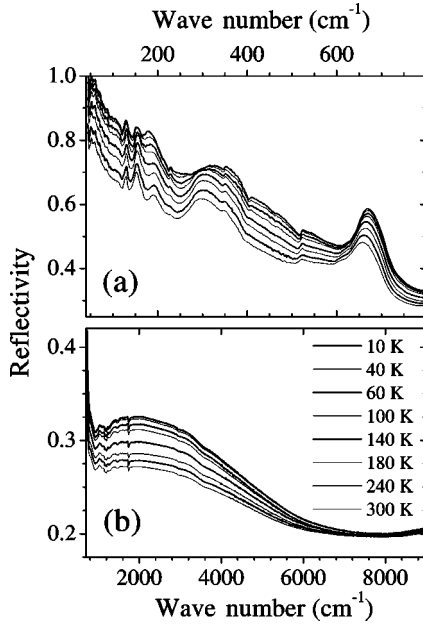
FIG. 1. Reflectivity spectra of Ru-1212 for different temperatures and for wave numbers (a) from 40 to 800 cm$^{-1}$ and (b) from 700 to 9000 cm$^{-1}$.
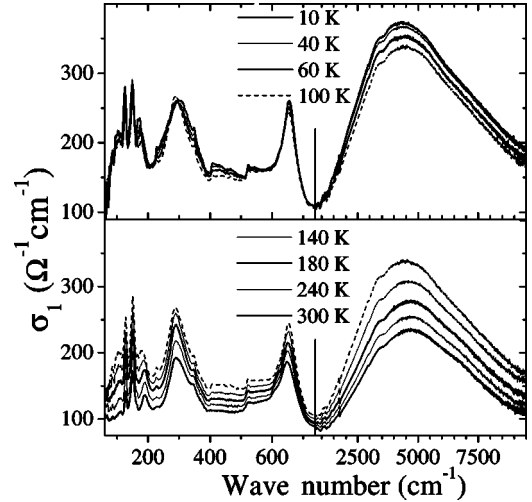


FIG. 2. Real part of the optical conductivity of Ru-1212 with $T_{SC} = 45$ K and $T_{FM} = 133$ K. Spectra are shown for $T = 10$, 40, 60, and 100 K—upper panels, and 100, 140, 180, 240, and 300 K—lower panels. Note the change of wave number scale from left to right panels.

$P4/mbm$ ($D_{4h}^5$) structure. The temperature-dependent magnetization[12] of the Ru-1212 samples reveals a magnetic transition temperature $T_M = 133$ K. A large value of diamagnetic shielding is seen below 28 K. The dc resistivity $\rho(T)$ is similar to that reported recently by Tallon *et al.*,[5] and shows the onset of a superconductivity at $T_{SC} = 45$ K with zero resistivity below 32 K. The temperature dependence of the resistitvity above $T_{SC}$ exhibits two different regimes with $d\rho/dT \lesssim 0$ for $T_{SC} < T < T^*$ and $d\rho/dT = \text{const} > 0$ for $T > T^*$ with a crossover temperature $T^* \simeq 90$ K.

Near-normal incidence reflectivities in the far-IR region from 30 to 750 cm$^{-1}$ were measured using a ''Bruker'' IFS 133v spectrometer with the newly designed Ge-coated 6 $\mu$m mylar beam splitter. This significantly increased the signal-to-noise ratio and avoided to merge the spectra at phonon frequencies. To extend the reflectivity measurements to higher frequencies, a ''Bruker'' IFS 66v/S spectrometer was used covering the frequency range from 600 to 16 000 cm$^{-1}$, the higher frequency limit being restricted by calibrating the reflectivity against the gold-coated sample. The sample was mounted in the ''Oxford Optistat'' He bath cryostat for the measurements from 10 to 300 K.

### III. EXPERIMENTAL RESULTS AND DISCUSSION

The reflectivity spectra of Ru-1212 for wave numbers up to 9000 cm$^{-1}$ and for different temperatures from 10 to 300 K are shown in Fig. 1. As the temperature decreases from 300 to 10 K, the reflectivity displays a gradual increase, consistent with an increase of the sample conductivity. Below the SC transition temperature the far-IR reflectivity is noticeably enhanced. This increase is reproducible and amounts to 3%. The reflectivity becomes close to unity at frequencies below 70 cm$^{-1}$ in the SC state. Comparing to the reflectivity spectra of Ru-1212 ceramics reported recently by Litvinchuk *et al.*,[13] our data show a noticeably higher (up to 10–20 %) reflectivity level in the spectral range under investigation. At all temperatures investigated five optical phonon modes near 128, 151, 190, 288, and 654 cm$^{-1}$ are clearly observed. It is well established[13–15] that the modes appearing in the spectra of anisotropic ceramics correspond to phonon modes polarized along the $c$ axis. The $ab$-plane response from phonons in the reflectivity spectra shown in Fig. 1(a) becomes apparent as additional small steplike features at 225, 352, and 520 cm$^{-1}$.

To obtain the optical conductivity via Kramers-Kronig analysis, we used a continuous low-frequency extrapolation of the reflectivity to $R(\omega = 0) = 1$, utilizing the formula $1 - \text{const} \, \omega^\gamma$, with $0.5 \leq \gamma \leq 2$. The lower and upper limits of $\gamma$ correspond to the Hagen-Rubens extrapolation for the normal state and the extrapolation for the SC state, respectively. However, there is no influence of the different extrapolations on the resulting optical conductivity for wave numbers $> 70$ cm$^{-1}$. For wave numbers higher than 16 000 cm$^{-1}$, an extrapolation using a $\omega^{-4}$ frequency dependence was used. The real part of the optical conductivity $\sigma_1(\omega)$ of Ru-1212 for different temperatures is shown in Fig. 2 (10 K $\leq T \leq 100$ K: upper panels; 100 K $\leq T \leq 300$ K: lower panels). At room temperature the five distinct IR-active phonon modes at 128, 151, 190, 288, and 654 cm$^{-1}$ are superimposed on a featureless electronic background of 100 $\Omega^{-1}$cm$^{-1}$, consistent with the room temperature dc conductivity value. The electronic background extends to higher frequencies and a broad mid-IR band appears at 4800 cm$^{-1}$.

The infrared-active phonons observed in the Ru-1212 ceramics (Fig. 2, left panels) can be assigned similarly as reported for the $c$-axis optical phonons in Y-123 crystals.[14–16] Indeed, Ru-1212 is structurally similar to the rare-earth cuprate superconductors such as Y-123 except that the Cu-O

chain layers are replaced by $RuO_2$ square planar layers. Ignoring the rotations of the $RuO_6$ octahedra, an approximate structure is then of tetragonal symmetry $P4/mmm$. A comparison with the IR spectra of Y-123 suggests that the phonon mode at 654 $cm^{-1}$ involves primarily the apical oxygen vibrations, whereas that at 288 $cm^{-1}$ is related to the Cu-O bending mode which involves vibrations of the oxygen ions of the $CuO_2$ planes. We suggest the three low-frequency modes at 128, 151, and 190 $cm^{-1}$ to be assigned to the displacements of Cu, Gd, and Ru, respectively. Indeed, the Cu-related mode at 128 $cm^{-1}$ is close in frequency to the in-plane Cu vibrations at 104 $cm^{-1}$ in Y-123 crystals. The eigenfrequency of the Gd mode at 151 $cm^{-1}$ agrees with that of rare-earth ($R$) related phonon mode in R-123 cuprates, where it is strongly $R$-dependent decreasing from 193 $cm^{-1}$ in Y-123 to 162 $cm^{-1}$ in Er-123 in accordance with the mass ratio of the $R$ ion. The assignment is confirmed by shell-model calculations for Ru-1212 with a $P4/mbm$ space group, reported recently by Litvinchuk et al.[13] These model calculations also suggest that the mode at 190 $cm^{-1}$ involves primarily Ru-ion vibrations against the Cu ions.

In order to determine the resonant frequencies of the observed phonon modes and the mid-IR band parameters at all temperatures, we applied a quantitative dispersion analysis by fitting both the reflectivity and optical conductivity spectra. The model dielectric function consists of a sum of Lorentzian functions, accounting for the contributions from the low-frequency phonon modes at 128, 151, and 190 $cm^{-1}$ and the mid-IR band as well. Additionally, the almost featureless electronic background at frequencies below 800 $cm^{-1}$ was included in a Kramers-Kronig consistent way into the fitting procedure using a sum of five broad Lorentzian bands with halfwidths more than 150 $cm^{-1}$. We have found that the two high-frequency phonon modes, mostly related to oxygen vibrations, are noticeably asymmetric in shape. The asymmetric phonon feature at 654 $cm^{-1}$ can be described by the Fano profile (see, e.g., Ref. 17), given by $\sigma(\omega) = i\sigma_0(q-i)^2(i+x)^{-1}$, with $x = (\omega^2 - \omega_T^2)/\gamma\omega$, $\gamma$ and $\omega_T$ are the linewidth and the resonant frequency, and $\sigma_0$ denotes the amplitude which is related to the oscillator strength as $S = 4\pi\sigma_0(q^2-1)\gamma\omega_T^{-2}$. The dimensionless Fano parameter $q = -1/\tan(\Theta/2)$ is a measure of the asymmetry of the peak and for $\Theta = 0$ a Lorentzian line shape is recovered. The asymmetry of the band at 654 $cm^{-1}$ yields $\Theta \sim 0.19$ at all temperatures in accordance with the Fano-profile description. A single resonance description fails for the strongly asymmetric phonon feature around 288 $cm^{-1}$, and we used two Lorentzian profiles to describe this band. The complex nature of the asymmetric structure involving the Cu-O bending mode at 288 $cm^{-1}$ will be verified by a detailed analysis of its temperature dependence.

Analyzing the temperature dependence of the optical conductivity of Ru-1212, we emphasize its striking resemblance of the $c$-axis conductivity of strongly underdoped SC Y-123 cuprates. Figure 3 shows the most apparent feature related to the onset of superconductivity which is the transformation of the bending mode at 288 $cm^{-1}$ [light solid curve in Fig. 3(a): $T = 100$ K] to a broad band centered at 308 $cm^{-1}$
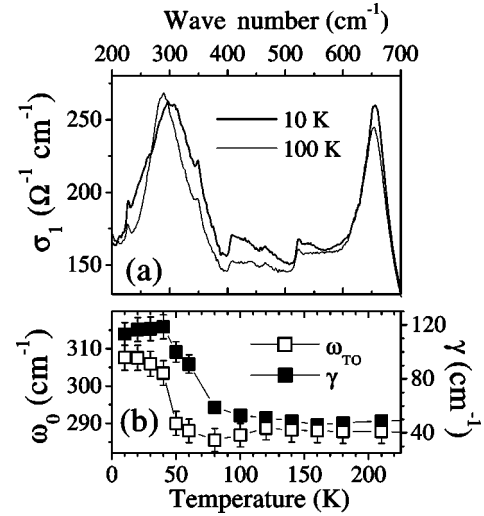


FIG. 3. (a) Real part of the optical conductivity at high-phonon frequencies at two different temperatures well above and well below $T_{SC} = 45$ K. (b) Temperature dependence of the position and the Lorentzian damping of the asymmetric peak at 288 $cm^{-1}$ (see text).

[heavy solid curve in Fig. 3(a): $T = 10$ K]. Figure 3(b) shows the detailed temperature dependence of the peak position of the asymmetric structure involving the 288 $cm^{-1}$ mode and of the Lorentzian damping factor of the fitting curve, which properly describes the low-frequency wing of the structure. The transformation of the band profile starts at around 90 K, close to $T^*$ defined above, being well below the magnetic transition temperature $T_M = 133$ K, but also well above $T_{SC} = 45$ K. The most pronounced changes are observed at $T_{SC}$, as can be clearly seen from the temperature dependence of the band position [open squares in Fig. 3(b)]. This behavior involving an anomaly of the Cu-O bending mode, accompanied by the formation of an additional broad absorption band at phonon frequencies, is well studied in the $c$-axis IR conductivity of underdoped layered cuprates.[10,11,18,19] The mechanism of this phenomenon is a subject of ongoing discussions.[8–10,19] The most favored explanation is based on a model where the bilayer cuprate compounds are treated as a superlattice of interbilayer and intrabilayer Josephson junctions.[8,10,11] In this model the additional absorption peak is related to the transverse bilayer plasmon, while the anomalous softening and the loss of the spectral weight of the Cu-O bending mode are explained to be due to the drastic changes of the local electrical fields acting on the in-plane oxygen ions as the Josephson current sets in. The gradual onset of the anomalies above $T_{SC}$ is explained due to the persistence of a coherent superconducting state within the individual copper-oxygen bilayers, whereas the steep and sudden changes at $T_{SC}$ occur when the macroscopically coherent superconducting state forms. This effect is strongly dependent on the doping level and is not observed in the optimally doped and overdoped Y-123 samples. For the strongly underdoped $YBa_2Cu_3O_{6.45}$, the transverse optical plasmon and the bending mode merge, forming a single highly asymmetric peak. Comparing the temperature dependence of the asymmetric peak in Ru-1212 at 288 $cm^{-1}$ with the data re-
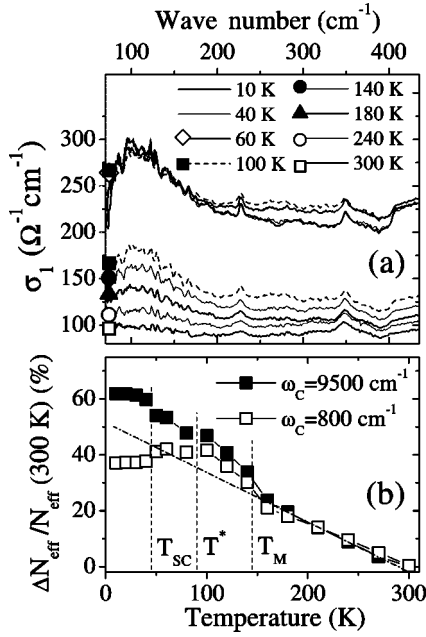
FIG. 4. (a) Temperature dependence of the electronic background far-IR conductivity with phonons being subtracted by fits to oscillators as described in the text. The curves for $T = 10$, 40, 60, and 100 K are shifted up by 100 $\Omega^{-1}\,cm^{-1}$ for clarity. The symbols on the $y$ axis represent the dc conductivity values. (b) Temperature dependences of $N_{eff}$ evaluated below $\omega_C$ and related to those at $T = 300$ K. The dot-dashed guideline continues the temperature dependences from above to below $T_M$.

$$N_{eff} = \frac{2 m_e V_{cell}}{\pi e^2} \int^{\omega_C} \sigma(\omega) d\omega, \tag{1}$$

where $\sigma(\omega)$ is the IR conductivity after subtraction of the phonons and the volume of the unit cell ($P4/mmm$) is $V_{cell} \simeq 1.7 \times 10^{-22}$ cm$^3$. The effective carrier densities with $\omega_C = 9500$ cm$^{-1}$ and $\omega_C = 800$ cm$^{-1}$ evaluated at 300 K are 0.12 and 0.005, respectively. As shown in Fig. 4(b), the temperature dependence of the LSW fully reproduces that of TSW for 300 K $\geqslant T \geqslant 100$ K. On further decreasing temperatures the TSW continues to increase, whereas the LSW remains constant or even slightly decreases. We suggest that the discrepancy in the temperature dependences of the LSW and TSW reflects the opening of the pseudogap in Ru-1212 superconductor. However, the effect is not very pronounced because of a significant contribution from the polaronlike mid-IR band to the LSW.

The mid-IR band reveals the shape and the energy scales typical of a small-polaron absorption. A clearly resolved maximum at 4800 cm$^{-1}$ at 300 K corresponds to a polaron binding energy of about 0.3 eV. The most remarkable features of this band are the anomalies which occur at the onset of ferromagnetic order within the Ru-O layers at $T_M = 133$ K, namely, the shift to lower energies from 4800 cm$^{-1}$ at $T = 180$ K to 4400 cm$^{-1}$ at $T = 50$ K and a strong increase in the SW. Figure 4(b) shows that the TSW contributed mainly from the mid-IR band increases continuously on decreasing temperature and reveals an anomaly at $T_M$, as indicated by a significant deviation from the guideline which roughly approximates the high-temperature dependence. The ferromagnetism in Ru-O layers is believed to have the same origin as in SrRuO$_3$, which, in turn, is explained by itinerant-electron ferromagnetism based on band theory.[22] The Ru ion in SrRuO$_3$ is in a tetravalent low-spin state $4d^{4+}: t_{2g}^3 \uparrow t_{2g}^1 \downarrow e_g^0$ ($S = 1$). The ferromagnetic coupling between Ru ions is transmitted via the itinerant electrons of the minority $t_{2g}$ band, the charge carrier transport being strongly dependent on the core spin alignment. In Ru-1212 the $t_{2g}$ minority band is partially occupied due to the hole doping of the CuO$_2$ biplanes resulting in weak itinerant ferromagnetism. Assuming that the mid-IR band is associated with the hopping conductivity of the minority $t_{2g}$ electrons, the strong carrier-spin interaction can naturally explain the temperature behavior of the band. As $T$ is decreased below $T_M$ the resulting onset of ferromagnetic correlations leads to an increase of the kinetic energy of the charge carriers, which, in turn, results in a decrease of the effective electron-phonon coupling. As a result, an increase in the TSW and a shift of the polaronic band to lower frequencies are observed. Note that this behavior of the SW is typical of magnetoresistive FM compounds such as the doped manganites,[23] and has been discussed in terms of a temperature-dependent competing effects between electron-phonon coupling and double-exchange interaction of core spins mediated by itinerant electrons.[24]

A further important feature associated with the magnetic transition in Ru-1212 is the anomalous shift of the Ru-related phonon mode at 190 cm$^{-1}$ as shown in Fig. 5(a). In Fig.

ported by Munzar *et al.* for YBa$_2$Cu$_3$O$_{6.45}$ (see Fig. 3 of Ref. 10) we find a striking similarity. The present observation suggests a strongly underdoped character of the weakly coupled cuprate biplanes and a strong anisotropy of the Ru-1212 compound. At the same time, the pronounced anomaly of the bending mode observed right at $T_{SC}$ implies that the Ru-1212 is a bulk superconductor at lower temperatures. This experimental evidence is important seeing the onset of a bulk superconductivity in Ru-1212 is still very much disputed.[2,21]

Another well-known feature of the underdoped cuprate superconductors is a suppression of spectral weight (SW) at low frequencies already above $T_{SC}$ due to the opening a normal state pseudogap.[20] This feature is not clearly observed in Ru-1212. On the contrary, as shown in the left panels of Fig. 2 the electronic background at low frequencies increases continuously as the temperature is lowered from 300 to 100 K, and remains almost constant below 100 K. The weak suppression in the electronic background conductivity below 400 cm$^{-1}$ for $T < 100$ K is shown in Fig. 4(a). However, the actual value of the effect depends on the assumptions made when the phonon-related features are subtracted. The relative suppression of the low frequency SW (LSW) evaluated below $\omega_C = 800$ cm$^{-1}$ becomes more evident when compared with the total SW (TSW) evaluated up to frequencies of $\omega_C = 9500$ cm$^{-1}$. Figure 4(b) shows the relative changes of the SW with decreasing temperature from 300 K, expressed in terms of the effective electron density per unit cell,
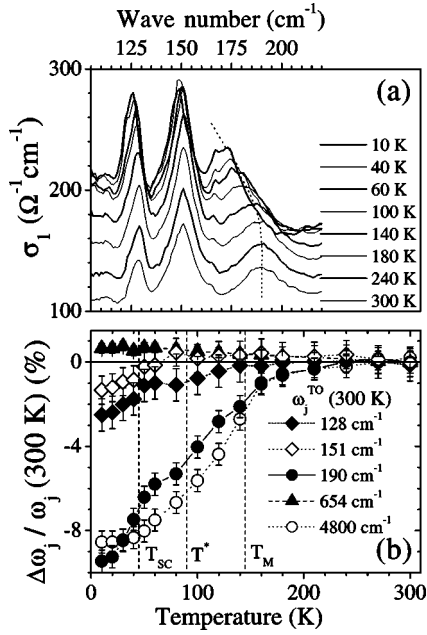
FIG. 5. (a) Real part of the optical conductivity at low phonon frequencies at different temperatures. The dotted line shows the temperature dependence of the eigenfrequency of the Ru-related mode derived by the dispersion analysis. (b) The relative shift of the resonant frequencies of the phonon modes and the mid-IR band observed on decreasing temperature from 300 K. The vertical dashed lines mark the critical temperatures.

5(b) we show the relative shifts of the low-frequency phonon modes at 128, 151, and 190 $cm^{-1}$ along with the shift of the apical oxygen phonon mode at 654 $cm^{-1}$ and the broad mid-IR band at 4800 $cm^{-1}$ observed on decreasing temperature from 300 K. Among all phonon modes, only the apical oxygen mode exhibits the classical inharmonic increase of the eigenfrequency on decreasing temperature, revealing anomalies neither at $T_{SC}$ nor at $T_M$. At the same time the low-frequency phonon modes show a characteristic softening at $T_{SC}$ as observed in Y-123 related compounds, and as discussed in terms of the resonance-frequency renormalization of the phonon modes lying below the SC gap.[14] However, the most pronounced effect is the anomalous softening of the mode at 190 $cm^{-1}$ which is related to the magnetic transition temperature in Ru-1212 compound, as shown in Fig. 5. The anomalous shift of the phonon mode at 190 $cm^{-1}$, reaching a relative value of 10% at the lowest temperatures, cannot be explained by structural changes of the bond lengths observed in Ru-1212,[4] all being less than 0.5%. This fact indicates that the Ru-related phonon mode is strongly affected by the interaction with the electronic system. It is important to note that the shifts of the phonon mode at 190 $cm^{-1}$ and the polaronic band at 4800 $cm^{-1}$ are apparently correlated, indicating a strong coupling of this phonon mode to the low-energy electronic excitations, as demonstrated in Fig. 5(b). The onset of this effect at the magnetic transition temperature and the decrease of the electron excitation energy on lowering temperature below $T_M$ can be explained by the renormalization of the electron-phonon coupling: The kinetic energy of the itinerant electrons increases

due to the onset of the ferromagnetic correlations in the Ru-O layers. This scenario can in turn explain the underdoped character of the stoichiometric Ru-1212 superconductor, where the strong hole depletion of the cuprate bilayers is caused by the charge carrier self-trapping on the Ru moments. We should note finally that as seen in Fig. 5(b), the 4800 $cm^{-1}$ band has the anomaly at $T_M$ on decreasing temperature with saturation below $T_{SC}$, while the 190 $cm^{-1}$ mode exhibits a singularity at about 90 K and further steep softening associated with the SC transition. This suggests that the bilayer plasmon-phonon coupling responsible for the anomaly of the Cu-O bending mode could also play a role in the softening of the 190 $cm^{-1}$ mode. To shed light on the origin of the predominant contribution, the detailed analysis of the mode eigenvectors is necessary, as well as of the temperature dependence of the oscillator strength and the damping factor. The accurate analysis of the temperature dependences will be possible after Ru-1212 single crystals have been prepared. On the other hand, the Ru-1212 system could provide an intriguing opportunity to develop the model of the bilayer Josephson plasmon for the case when a ferromagnetic moment is in the insulating plane. Further investigations of the effect of applying an external magnetic field on the interbilayer coupling and the related phonon anomalies are very promising.

## IV. CONCLUSIONS

In conclusion, we have investigated the optical conductivity of Ru-1212. The transformation of the Cu-O bending phonon mode at 288 $cm^{-1}$ in the normal state to an absorption band at 308 $cm^{-1}$ in the SC state has been observed. This observation strikingly resembles data reported recently for the strongly underdoped $YBa_2Cu_3O_{6.45}$ crystals, which were explained with a model invoking the onset of interbilayer and intrabilayer Josephson junctions. The present observation evidences a strongly underdoped character of the bulk superconductivity originated in weakly coupled cuprate biplanes. The optical conductivity of Ru-1212 is discussed in terms of a two-fluid model, the far-IR and dc conductivity being predominantly associated with the conductivity in the $CuO_2$ planes, whereas the mid-IR conductivity being associated with the hopping conductivity in the Ru-O layers. The correlated anomalous shifts of the Ru-related phonon mode at 190 $cm^{-1}$ and the polaron band at 4800 $cm^{-1}$ to lower frequencies have been observed on decreasing temperature below the $T_M = 133$ K. The underdoped character of the stoichiometric Ru-1212 superconductor is explained by the strong hole depletion of the cuprate bilayers caused by the charge carrier self-trapping on the Ru moments.

[1] C. Bernhard, J.L. Tallon, Ch. Niedermayer, Th. Blasius, A. Golnik, E. Brücher, R.K. Kremer, D.R. Noakes, C.E. Stronach, and E.J. Ansaldo, Phys. Rev. B **59**, 14 099 (1999).

[2] C. Bernhard, J.L. Tallon, E. Brücher, and R.K. Kremer, Phys. Rev. B **61**, R14 960 (2000).

[3] A.C. McLaughlin, W. Zhou, J.P. Attfield, A.N. Fitch, and J.L. Tallon, Phys. Rev. B **60**, 7512 (1999).

[4] O. Chmaissam, J.D. Jorgensen, H. Shaked, P. Dollar, and J.L. Tallon, Phys. Rev. B **61**, 6401 (2000).

[5] J.L. Tallon, J.W. Loram, G.V.M. Williams, and C. Bernhard, Phys. Rev. B **61**, R6471 (2000).

[6] J.W. Lynn, B. Keimer, C. Ulrich, C. Bernhard, and J.L. Tallon, Phys. Rev. B **61**, R14 964 (2000).

[7] G.V.M. Williams and S. Krämer, Phys. Rev. B **62**, 4132 (2000).

[8] M. Grüninger, D. van der Marel, A.A. Tsvetkov, and A. Erb, Phys. Rev. Lett. **84**, 1575 (2000).

[9] L.B. Ioffe and A.J. Millis, Phys. Rev. B **61**, 9077 (2000).

[10] D. Munzar, C. Bernhard, A. Golnik, J. Humlíček, and M. Cardona, Solid State Commun. **112**, 365 (1999).

[11] C. Bernhard, D. Munzar, A. Golnik, C.T. Lin, A. Wittlin, J. Humlíček, and M. Cardona, Phys. Rev. B **61**, 618 (2000).

[12] J. Hemberger, P. Mandal, A. Hassen, A.V. Boris, K. Pucher, A. Pimenov, and A. Loidl (unpublished).

[13] A.P. Litvinchuk, M.N. Iliev, Y.-Y. Xue, R.L. Meng, C.W. Chu, and V.N. Popov, Phys. Rev. B **62**, 9709 (2000).

[14] A.P. Litvinchuk, C. Thomsen, and M. Cardona, in *Physical Properties of High Temperature Superconductors IV*, edited by D.M. Ginsberg (World Scientfic, Singapore, 1994), p. 375, and references therein.

[15] R. Henn, T. Strach, E. Schönherr, and M. Cardona, Phys. Rev. B **55**, 3285 (1997).

[16] J. Schützmann, S. Tajima, S. Miyamoto, Y. Sato, and R. Hauff, Phys. Rev. B **52**, 13 665 (1995).

[17] A. Damascelli, K. Skulte, D. van Marel, and A.A. Menovsky, Phys. Rev. B **55**, R4863 (1997).

[18] C.C. Homes, T. Timusk, D.A. Bonn, R. Liang, and W.N. Hardy, Physica C **254**, 265 (1995).

[19] R. Hauff, S. Tajima, W.-J. Jang, and A.I. Rykov, Phys. Rev. Lett. **77**, 4620 (1996).

[20] Tom Timusk and Bryan Statt, Rep. Prog. Phys. **62**, 61 (1999).

[21] Jian-Xin Zhu, C.S. Ting, and C.W. Chu, Phys. Rev. B **62**, 11 369 (2000).

[22] S.C. Gausepohl, Mark Lee, K. Char, R.A. Rao, and C.B. Eom, Phys. Rev. B **52**, 3459 (1995); I.I. Mazin and D.J. Singh, *ibid.* **56**, 2556 (1997); J.S. Dodge, E. Kulatov, L. Klein, C.H. Ahn, J.W. Reiner, L. Miéville, T.H. Geballe, M.R. Beasley, A. Kapitulnik, H. Ohta, Yu. Uspenskii, and S. Halilov, *ibid.* **60**, R6987 (1999).

[23] A.V. Boris, N.N. Kovaleva, A.V. Bazhenov, P.J.M. van Bentum, Th. Rasing, S-W. Cheong, A.V. Samoilov, and N.-C. Yeh, Phys. Rev. B **59**, R697 (1999).

[24] A.J. Millis, R. Mueller, and Boris. I. Shraiman, Phys. Rev. B **54**, 5405 (1996); A. Chattopadhyay, A.J. Millis, and S. Das Sarma, *ibid.* **61**, 10 738 (2000).